PL-TR-
95-1140

FIELD EXPERIMENTAL RESULTS USING PHASE DIVERSITY ON A BINARY STAR

Richard A. Carreras
Sergio R. Restaino

May 1996

Final Report

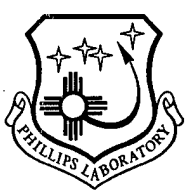

PHILLIPS LABORATORY
Lasers and Imaging Directorate
AIR FORCE MATERIEL COMMAND
KIRTLAND AIR FORCE BASE, NM 87117-5776

DISCLAIMER NOTICE

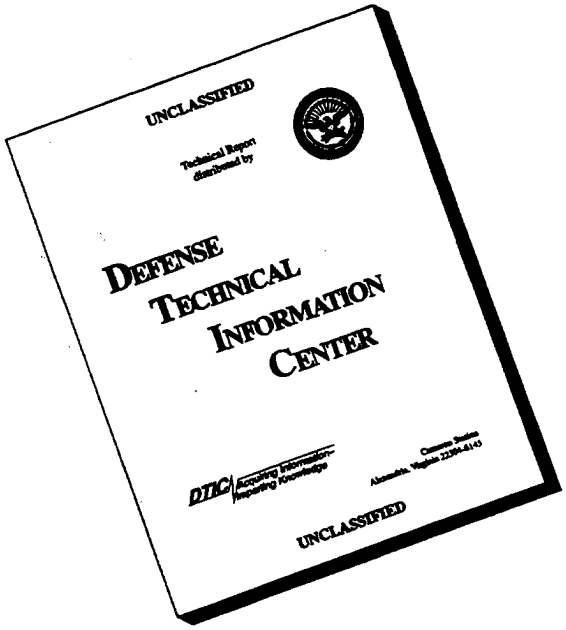

THIS DOCUMENT IS BEST QUALITY AVAILABLE. THE COPY FURNISHED TO DTIC CONTAINED A SIGNIFICANT NUMBER OF PAGES WHICH DO NOT REPRODUCE LEGIBLY.

Using Government drawings, specifications, or other data included in this document for any purpose other than Government procurement does not in any way obligate the U.S. Government. The fact that the Government formulated or supplied the drawings, specifications, or other data, does not license the holder or any other person or corporation; or convey any rights or permission to manufacture, use, or sell any patented invention that may relate to them.

This report has been reviewed by the Public Affairs Office and is releasable to the National Technical Information Service (NTIS). At NTIS, it will be available to the general public, including foreign nationals.

If you change your address, wish to be removed from the mailing list, or your organization no longer employs the addressee, please notify PL/LIMS, 3550 Aberdeen Ave SE, Kirtland AFB, NM 87117-5776.

Do not return copies of this report unless contractual obligations or notice on a specific document requires its return.

This report has been approved for publication.

Richard A. Carreras

RICHARD A. CARRERAS
Project Officer

FOR THE COMMANDER

C. DeHainaut

DR CHRISTOPHER R. DEHAINAUT
Chief, Remote Sensing Branch

ROBERT A. DURYEA, Col, USAF
Director, Lasers and Imaging
Directorate

1. Report Date (dd-mm-yy) 30 May 96	2. Report Type Final	3. Dates covered (from... to) May 94- Nov 95
4. Title & subtitle FIELD EXPERIMENTAL RESULTS USING PHASE DIVERSITY ON A BINARY STAR		5a. Contract or Grant #
		5b. Program Element # 63605F
6. Author(s) Richard A. Carreras Sergio R. Restaino		5c. Project # 3326
		5d. Task # LJ
		5e. Work Unit # 17
7. Performing Organization Name & Address Phillips Laboratory Lasers and Imaging Directorate/LIMS 3550 Aberdeen Ave SE, Bldg 499 Kirland AFB, NM 87117-5776		8. Performing Organization Report # PL-TR-95-1140
9. Sponsoring/Monitoring Agency Name & Address		10. Monitor Acronym
		11. Monitor Report #
12. Distribution/Availability Statement Approved for public release; distribution is unlimited.		
13. Supplementary Notes		

14. Abstract This report describes the optical imaging of a binary star using a phase diversity technique. The two stars of the binary star μ Scorpio, with a separation of 1.1 arc seconds, were successfully resolved. The data was taken at the Air Force Maui Optical Site (AMOS) atop Mount Haleakala, Maui, Hawaii, using the 81 centimeter, Beam Director Telescope (BDT). First, a detailed theoretical description of phase diversity to lay the foundations for the experimental effort is presented. Then the phase diversity algorithm is formulated in the context of nonlinear programming where a metric is developed and then minimized. We solve for the Zernike coefficients directly using nonlinear optimization techniques. Detailed discussion of the experimental implementation is described. Phase diversity was used on in-focus and out-of-focus images to extract the complete system Optical Transfer function (OTF). Finally, a parametric Wiener filter was used to get the final reconstructed image.

15. Subject Terms Phase Diversity, Wavefront Sensors, Active Phasing, Point Control, Telescope Control Loops, Optical Control Loops, Optical Position Control

Security Classification of			19. Limitation of Abstract	20. # of Pages	21. Responsible Person (Name and Telephone #)
16. Report Unclassified	17. Abstract Unclassified	18. This Page Unclassified	Unlimited	22	Richard A. Carreras (505)853-3258

TABLE OF CONTENTS

FIGURES

Field Experimental Results Using Phase Diversity on a Binary Star

Richard A. Carreras, Sergio Restaino

PL/LIMI Imaging Technologies Branch
U.S. Air Force, Phillips Laboratory
3550 Aberdeen Av. SE
Kirtland AFB, New Mexico, 87117-5776

1.0 INTRODUCTION

Many scientists and engineers have been interested in understanding and then improving the process of image formation. Obtaining any improvement is especially challenging when something in the image formation process corrupts the image. This requires a good understanding of the image formation processes, including which processes degrade the image. Once an accurate understanding of such processes is acquired, the scientists and engineers have an opportunity to use image reconstruction and image deconvolution to obtain better images. Phase Diversity affords the researcher the ability to fully characterize the aberrations which caused the degradation. Therefore, it is obvious that the better the degrading process is characterized, the more success one will have in undoing the process to recover a more accurate image.

Image degradations occur in a variety of imaging systems including photography, industrial radiography, mircoscophy, medical imaging, remote sensing, aerial reconnaissance, ground-based imaging and space-based imaging[1]. Fortunately, a few types of degradation phenomena appear repeatedly, therefore, good system and degradation models have been developed. Descriptions of the models are needed to mathematically characterize the image formation process.

The technique known as Phase Diversity can be viewed as a wavefront sensor which detects the phase aberrations from image data. This technique requires the collection of two or more images. The first image is the typical image collected referred to as the focal plane image, which has been degraded by the unknown aberrations. The additional images of the same object are formed by

inducing a known aberration onto the same focal plane image. For this article there is only one additional image besides the focal plane image which is needed, and is referred to the diverse image. This image will use focus as the known aberration, although the induced aberration is not limited to focus. It could be any other known aberration such as spherical or coma. The key is that this induced aberration must be exactly known. Therefore, focus was a likely candidate since it is easily induced and measured. Thus, the first image is the best in focused image which can be collected. The second image is the same as the first with the addition of a known focus aberration.

There are several advantages to the technique of Phase Diversity, the first advantage is its simplicity in implementation. The technique only requires a beam splitter and a prism to implement. Both the in focus and the out of focus images can be collected on the same camera. Thus, this simple configuration requires less maintenance and overhead. A second advantage is the fact that Phase Diversity as a wavefront sensor can detect a piston error between two adjacent telescopes, thus, is useful in phased array telescopes and interferometer designs. Other wavefront sensors such as the Shack-Hartman or shearing interferometer wavefront sensors are not able to detect piston. Phase Diversity also relies on an external, common reference, that of the object, which makes the techniques more robust, and less susceptible to systematic errors induced by optical hardware. Phase Diversity also performs well with extended objects. With little changes to the optical system Phase Diversity has the advantage of having a variable sensitivity control. Finally, Phase Diversity uses each photon to form the image and to do aberration detection. This could be an advantage over standard wavefront sensing techniques which split the valuable photons from the image to a separate wavefront sensor to perform the aberration detection[2].

2.0 PROBLEM SETUP

The framework for the development of the mathematical model requires the assumptions that the system be continuous, linear, and shift invariant. The imaging system used here is shown in Figure(1). All variables shown in Figure(1) are in the spatial domain, where $o(x,y)$ is the original object and can be seen to go in two directions. The top direction is to the in-focus optical system and

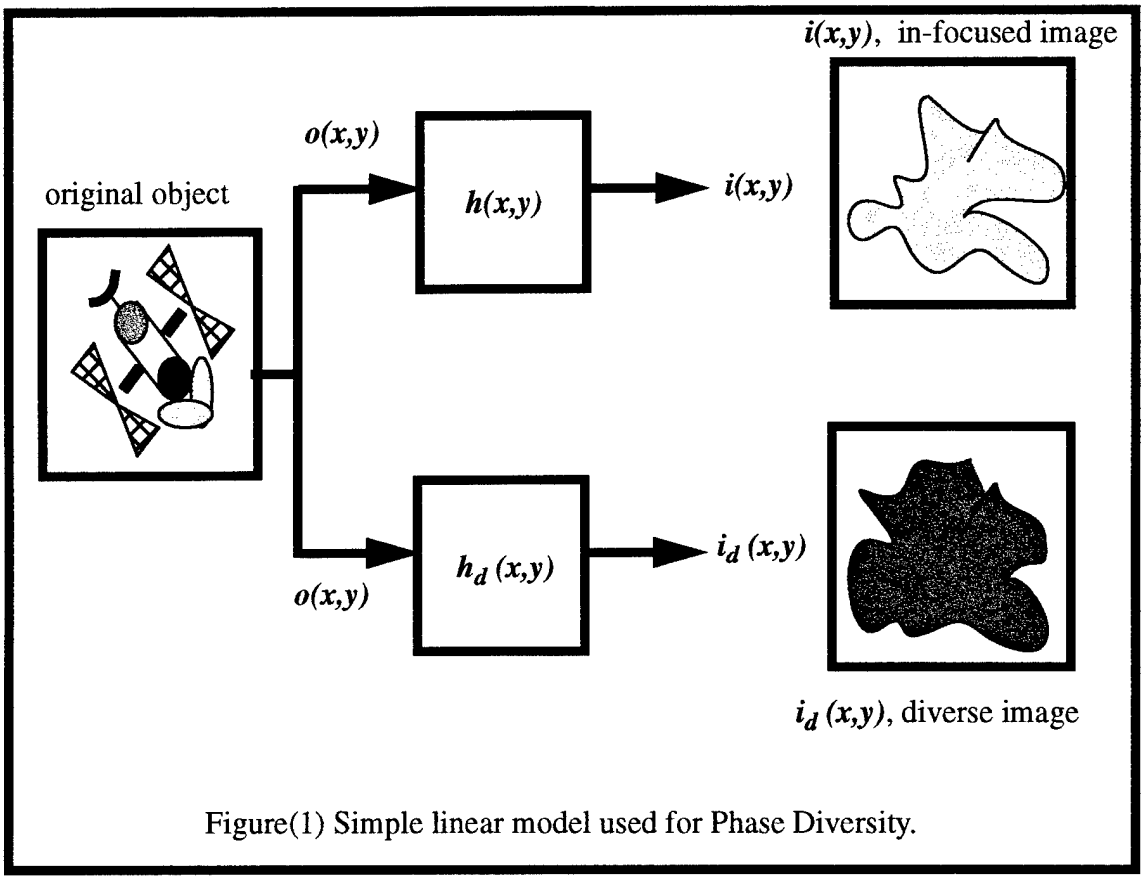

Figure(1) Simple linear model used for Phase Diversity.

the bottom direction is to the out of focus, diverse optical system. Now, $i(x,y)$ is the received image from the in-focus optical system, similarly, $i_d(x,y)$ is the diverse image from the out of focus optical system. Next, $h(x,y)$ is the point spread function (PSF) for the in-focus optical system and $h_p(x,y)$ is the point spread function of the out of focus optical system. For this particular model, the box in Figure(1) labeled $h(x,y)$ is a model that represents both the optical imaging system, and the propagation medium, under the aforementioned assumptions.

The input output relationship for the in focus optical system is described by the following equation[3,4],

$$i(x, y) = o(x, y) * h(x, y) . \tag{1}$$

The equation in the Fourier domain is the following,

$$I(u, v) = O(u, v) H(u, v) . \tag{2}$$

Where $I(u,v)$ is the Image spectra; $O(u,v)$ is the object spectra; and $H(u,v)$ is the Optical Transfer Function (OTF). The OTF, is defined as the following autocorrelation.

$$H(u,v) = P(u,v) \oplus P(u,v) \tag{3}$$

Where $P(u,v)$ is referred to as the generalized pupil function and is defined as the following equation,

$$P(u,v) = A(u,v)\, e^{i\phi(u,v)}. \tag{4}$$

The $A(u,v)$ is defined as the pupil function of the optical system and $\phi(u,v)$ can be expanded in a series as follows.

$$\phi(u,v) = \sum_{n=1}^{N} \alpha_1 + \alpha_2\cos\theta + \alpha_3\sin\theta + \alpha_4 R^2 + \alpha_5 R^2\cos 2\theta + \alpha_6 R^2\sin(2\theta) + \ldots\ldots + \alpha_n func(R,\theta) \tag{5}$$

The $\phi_n(u,v)$ is the basis function used in optics to describe the various aberrations and it is composed of the discretized Zernike polynomials. The Zernike coefficients are the α_n in front of each polynomial function, where α_1 is piston coefficient, α_2 and α_3 are x-tilt and y-tilt coefficients, α_4 is focus coefficients, etc. The following definitions are used for R and θ,

$$R = \sqrt{u^2 + (v)^2} \quad \text{and} \quad \theta = \text{atan}\left(\frac{v}{u}\right). \tag{6}$$

The following are the corresponding companion equations for the defocused, diverse system:

$$i_d(x,y) = o(x,y) * h_d(x,y), \tag{7}$$

$$I_d(u,v) = O(u,v)\, H_d(u,v), \tag{8}$$

$$H_d(u,v) = P_d(u,v) \oplus P_d(u,v). \tag{9}$$

Where the generalized pupil function for the diverse system is the following equation.

$$P_d(u,v) = A(u,v)\, e^{i\{\phi(u,v) + \Delta\varepsilon(u,v)\}} \tag{10}$$

Notice that the generalized pupil function for the diverse optical system has the known defocus term added to the exponential and is designated as $\Delta\varepsilon(u,v)$.

Now starting with two basic equations in the frequency domain for the in-focus and diverse optical systems,

$$I(u,v) = O(u,v)H(u,v), \tag{11}$$

$$I_d(u,v) = O(u,v)H_d(u,v). \tag{12}$$

Both $I(u,v)$ and $I_d(u,v)$ are computed by the measured image data. $H(u,v)$, $H_d(u,v)$ and $O(u,v)$ are unknowns. Setting up an error metric between the measured and diverse images to get the following equation,

$$E = \sum_u \sum_v \left| I(u,v) - O(u,v)H(u,v) \right|^2 + \sum_u \sum_v \left| I_d(u,v) - O(u,v)H_d(u,v) \right|^2. \tag{13}$$

Now take the derivative of the above error metric (E) with respect to the object, $O(u,v)$ and set equal to zero, then solve for $O(u,v)$. After some algebraic manipulations $O(u,v)$ is found as a function of $H(u,v)$, $H_d(u,v)$, $I(u,v)$ and $I_d(u,v)$,

$$O(u,v) = \frac{H^*(u,v)I(u,v) + H_d^*(u,v)I_d(u,v)}{\left|H(u,v)\right|^2 + \left|H_d(u,v)\right|^2}. \tag{14}$$

Substituting this equation into the above error metric with appropriate algebraic manipulations yields the following equation.

$$E = \sum_u \sum_v \frac{\left| I(u,v)\hat{H}_d(u,v) - I_d(u,v)\hat{H}(u,v) \right|^2}{\left|\hat{H}(u,v)\right|^2 + \left|\hat{H}_d(u,v)\right|^2}. \tag{15}$$

Remarkably, this expression is independent of the original object estimate $O(u,v)$ and was first derived by Gonsalves[5,6]. Throughout the rest of this article this equation is referred to as the Gonsalves error metric.

Given the above error metric, a possible strategy is to minimize the Gonzalves error metric, by the estimation of the coefficients of the Zernike polynomials in Equation (5), from which the estimate of both OTF's (i.e. $\hat{H}(u,v)$ and $\hat{H}_d(u,v)$) can be calculated. The minimization can be accomplished by using nonlinear optimization techniques, such as conjugate gradient or simplex algorithms. The conjugate gradient was chosen as the nonlinear optimization algorithm since it is well understood, is fast, and its memory requirements are workable. In addition there are many conjugate gradient routines which are available in various scientific software packages. The conjugate gradient used for this research is from the IMSL libraries and uses finite difference methods to calculate the gradient.

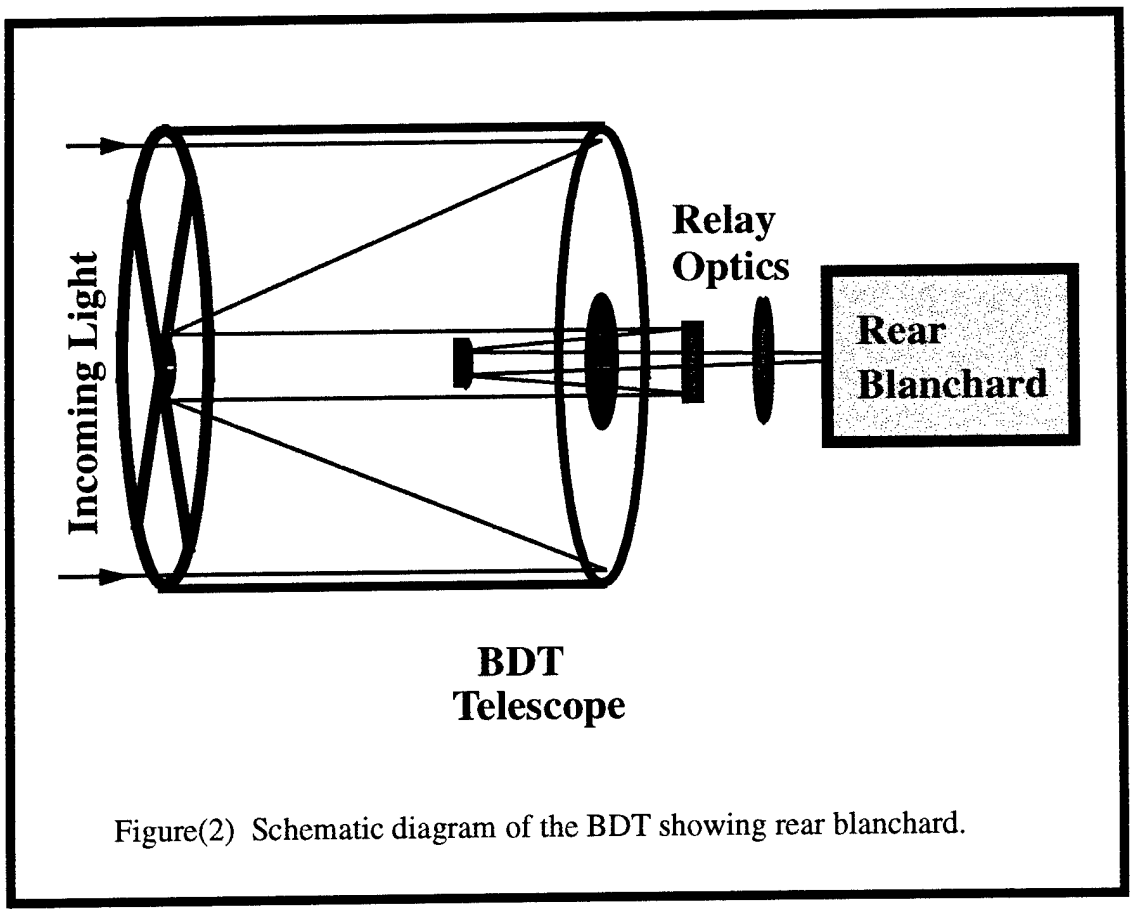

Figure(2) Schematic diagram of the BDT showing rear blanchard.

3.0 EXPERIMENTAL SETPUT

It was desired to acquire data of an astrological source in order to test the Phase Diversity algorithm under actual field conditions. The site which was chosen had a small 32 inch, (81 centimeter) Mersenne-Cassegrain Telescope which was available for the experiment. The telescope is called the Beam Director Telescope (BDT) and is located at the Air Force Maui Optical Site (AMOS) atop of mount Haleakela, in Maui, Hawaii. The telescope had a rear blanchard on which the Phase Diversity hardware could be attached. In addition the telescope has the capability to track near-earth objects when necessary. The telescope diagram is shown in Figure (2), with the blanchard shown at the back of the telescope.

The rear blanchard is shown in greater detail in Figure (3). The relay optics are generically shown as the lens L2. The next lens on the beam train is L3 which is the focusing lens which focuses the beam onto the camera. The camera chosen for the experiment was a SpectraSource Instruments, model MCD1000, with a grade zero, 768X512 Kodak KAF-0400 silicon CCD sensor. This camera is an astronomical quality camera with no bad pixels, high sensitivity and low read out noise. In addition, this camera was chosen because of its software interface to a PC-type computer being very flexible This software was easily modified to perform the type of tasks necessary for viewing fast, near-earth objects when necessary. This flexibility was exercised in the size of data frame collected for the Phase Diversity experiment; the camera was set to have an active window of 64X128 pixels, all other pixels were turned off.

Early in the experiment planning it was decided to try to get both the in focus and out of focus images on the same camera, as opposed to using two cameras, thus, conserving space in the telescope rear blanchard. This is reflected in the optical design where the two images are created with the combination turning flat mirror and beam splitter in Figure (3). This beam splitter/mirror combination create the in focus and the out of focus images. This is done because the beam splitter reflects 40 percent of the incoming light into the CCD camera. This first reflection is the in focus

image. The other 60 percent is transmitted through onto the mirror. The mirror reflects the entire 60 percent of the transmitted light. This reflected light has to go through the beam splitter again, and only 60 percent of this reflected light gets through. This leaves 36 percent of the original light going toward the camera to form the out of focus image. This image is out of focus due to the extra length which this path traversed through the beam splitter, off the mirror and through the beam splitter again. The exact distance could be controlled using different spacers between the beam splitter and the mirror. The width of the spacers were calculated to give a defocus of one wave, taking the f-number of the focusing lens into consideration. In summation, the in focus image has 40 percent of the original light coming in and the out of focus image has 36 percent of the original light.

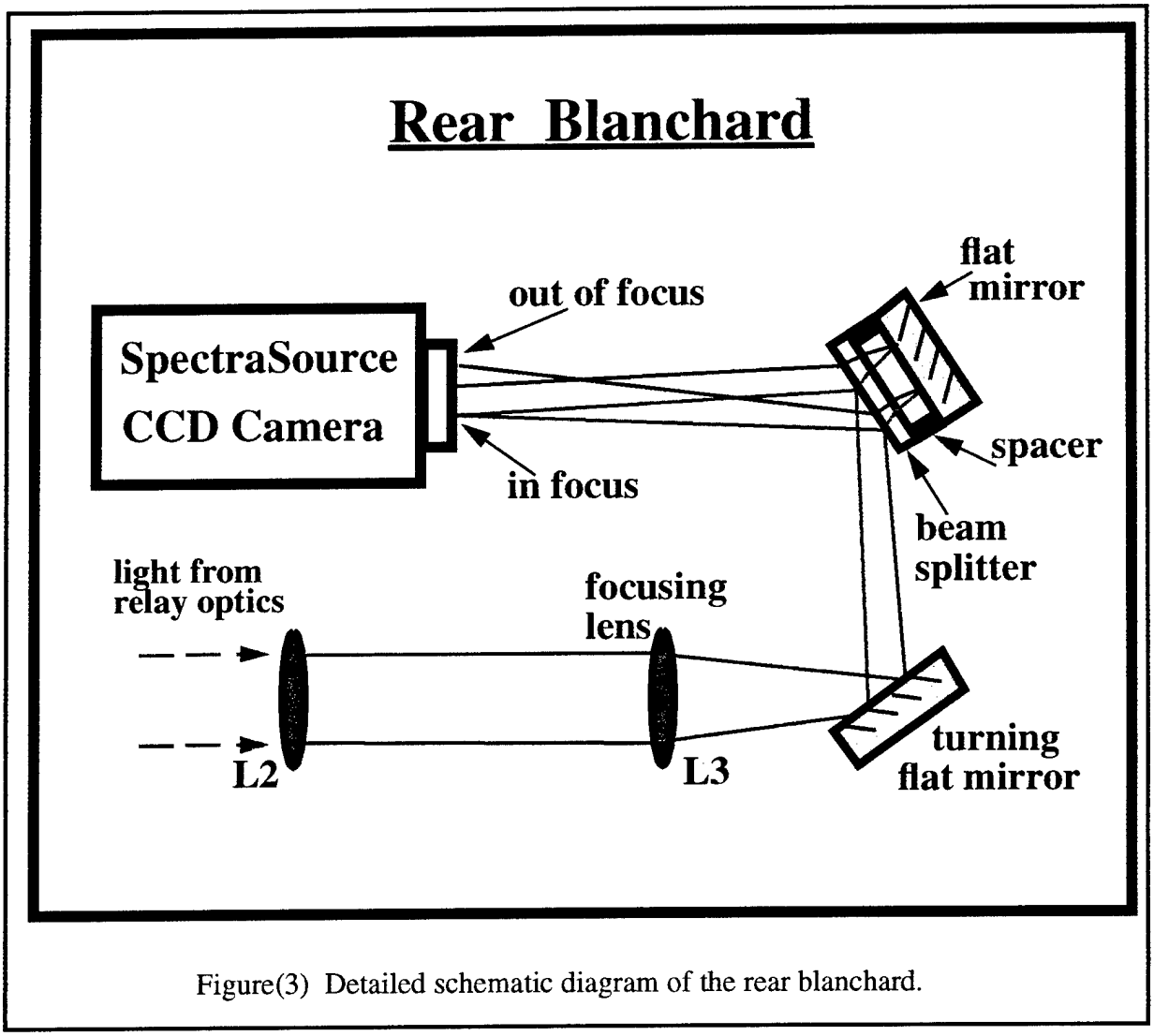

Figure(3) Detailed schematic diagram of the rear blanchard.

The in focus and out of focus images were desired to be side by side. Thus, the dimension of the camera window selected was 64 pixels high and 128 pixel wide. Figure (4) shows a typical camera frame of data taken of the binary star μ Scorpio. In addition the optical design was calculated to give a pixel to pixel separation of 0.1 arcseconds.

4.0 EXPERIMENTAL RESULTS

As can be seen from the data in Figure (4), the in focus image is on the right side and the out of focus is on the left side. The two images were offset slightly in the vertical direction, such that if there were and ghosting or aliasing due to the brightest pixel on one side it would not influence the adjacent image. Therefore, the out of focus image on the left is slightly higher on the camera area

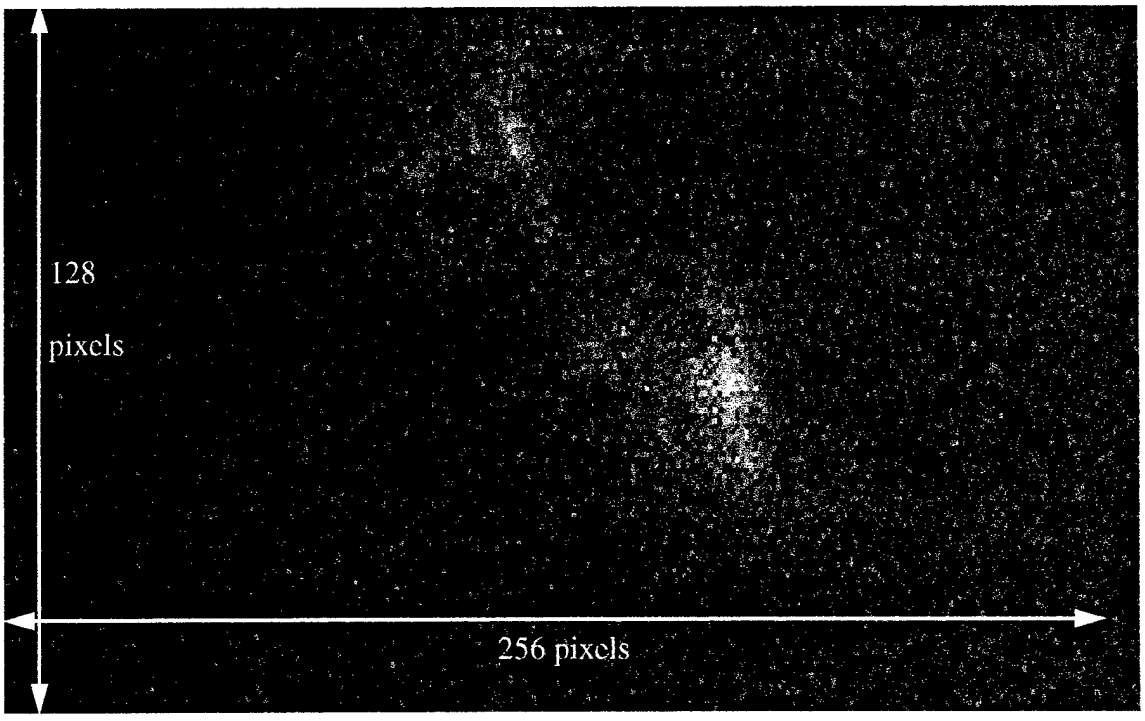

Figure(4) Single camera frame of in focus and out of focus images.

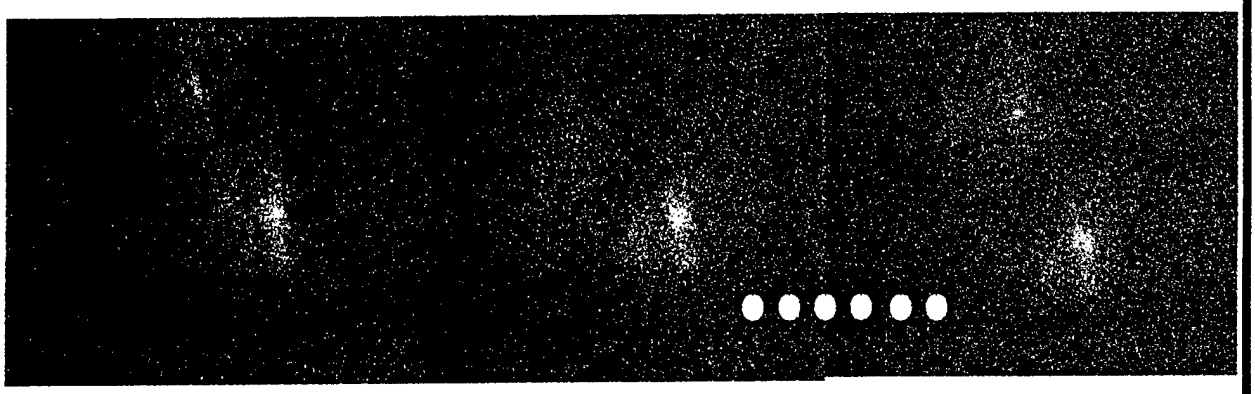

Frame #1 **Frame #2 ● ● ● ● ● ● Frame #300**

Figure(5) 300 frames of data with 50 msec exposure times.

than the in focus image. In order to freeze the atmosphere the frames were taken at 50 msec exposure rates. For this data set there were 300 frames of data taken of μ Scorpio.

As can be seen from Figure (4), the quality of data is marginal since the Signal to Noise is low. This is a function of the amount of light during the exposure time allotted. Doing Phase Diversity on these individual frames would have been difficult. Therefore, in an effort to improve the Signal to Noise of the in focus image and the out of focus image, the 300 frames were averaged. A 64X64 pixel cutout of the in focus image and a 64X64 pixel cutout of the out of focus image were taken from each of the 300 frames, as shown in Figure(5). All the 64X64 in focused images were average and centroided in the frequency domain, as were the out of focused images. The averaged images were inverse Fourier transformed in order to show the results. The results are shown in Figure (6).

The Fourier spectra of the averaged images were then used in the Phase Diversity algorithm discussed in section 2.0. Recall the method was to minimize the Gonzalves error metric, Equation (15), by the estimation of the coefficients of the Zernike polynomials in Equation (5), from which the estimate of both OTF's (i.e. $\hat{H}(u,v)$ and $\hat{H}_d(u,v)$) is calculated. The minimization was

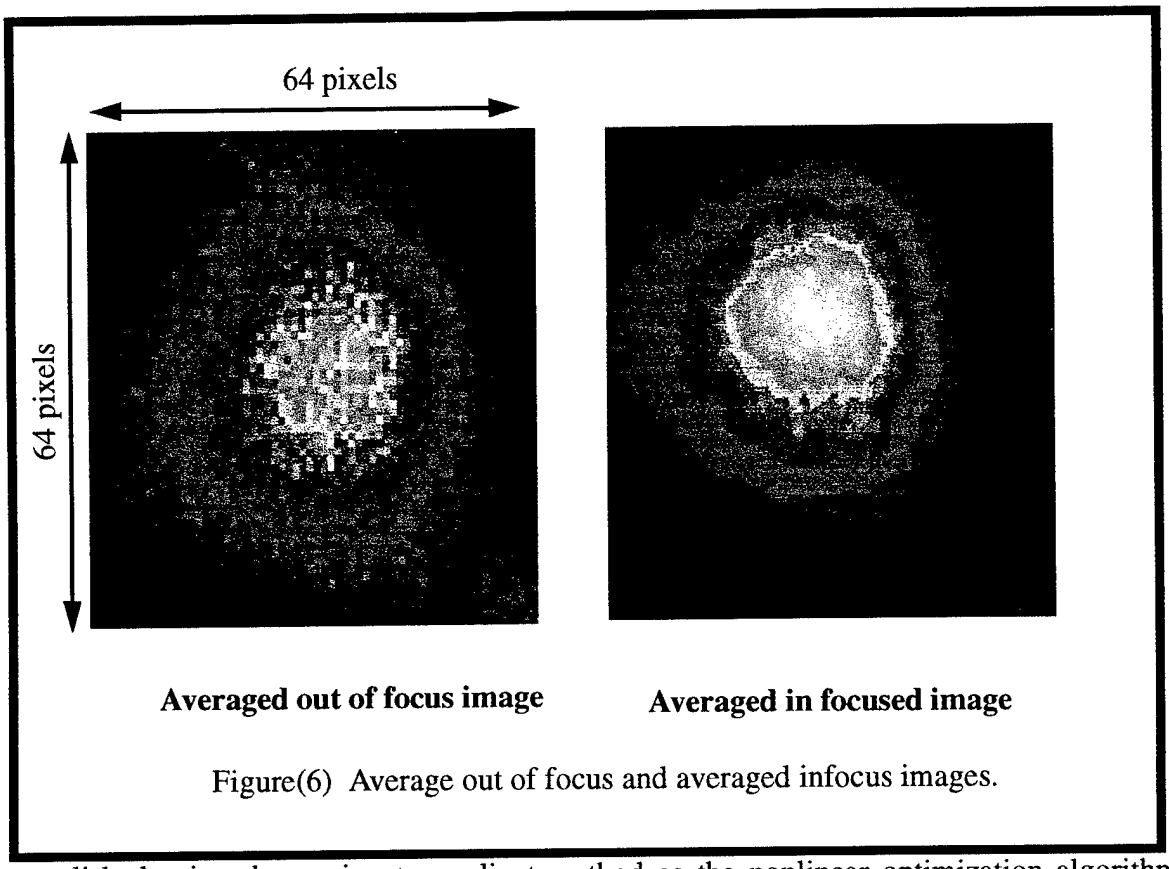

Figure(6) Average out of focus and averaged infocus images.

accomplished using the conjugate gradient method as the nonlinear optimization algorithm. The conjugate gradient used on this data is from the IMSL libraries which uses finite difference methods to calculate the gradient.

The estimate of the in focus OTF ($\hat{H}(u,v)$), was constructed after the Zernike coefficients were calculated. The modulus of the calculated OTF (i.e. the Modulation Transfer Function (MTF)) is shown in Figure (7). This is the OTF for the entire optical system including the atmospheric aberrations. From this estimated OTF the in focus image was used in a parametric Wiener filter to perform the image recovery. Recall the parametric Wiener filter is of the form shown in Equation (16).

$$\hat{O}(u,v) = \frac{\langle \hat{H}(u,v) \rangle^{*} \langle I(u,v) \rangle}{\left| \langle \hat{H}(u,v) \rangle \right|^{2} + \beta \left[\frac{1}{\langle SNR(u,v) \rangle} \right]} \tag{16}$$

Where the Signal to Noise $SNR(u,v)$ can be calculated from the ensemble of data of the in focus image spectra.

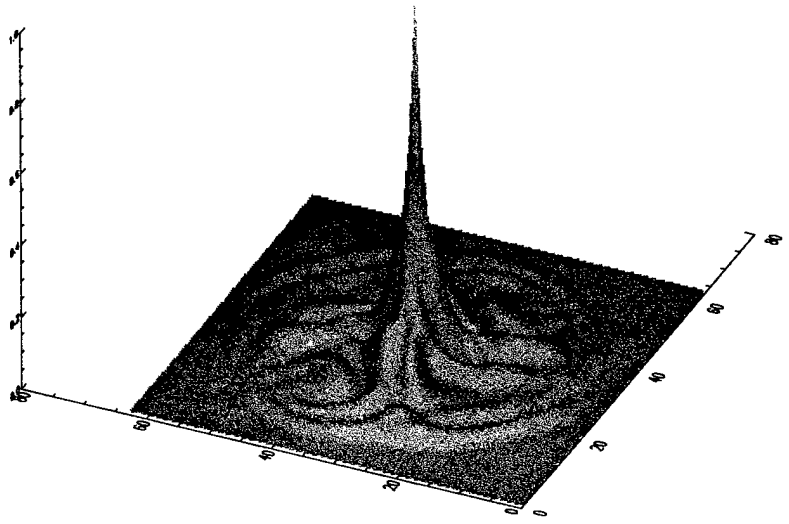

Figure(7) Estimated Modulation Transfer Function (MTF).

The results from the deconvolution of the Wiener filter are shown in Figure (8). The averaged in focus image is again shown for comparison. The vast improvement from the averaged image on the left to the deconvolved object on the right is quite dramatic. The two stars of the binary star system of μ Scorpio can be easily seen. In order to verify more precise characteristics of this binary star, μ Scorpio was found in an astronomical catalog. It was listed as having an angular separation of 1.1 arcseconds and a difference of relative magnitude of 2.5 between the brighter star and the dimmer star. Recall the camera and associated optics was set to have an angular separation of 0.1 arcseconds per pixel. In order to verify these characteristics, the deconvoled object was magnified, as seen as the last image on Figure (8). It is seen that approximately 11 pixels separate the centers of the stars, which corroborates the stellar catalog. In addition the brightest star was found to be approximately 2 and a half times brighter that the dimmer star.

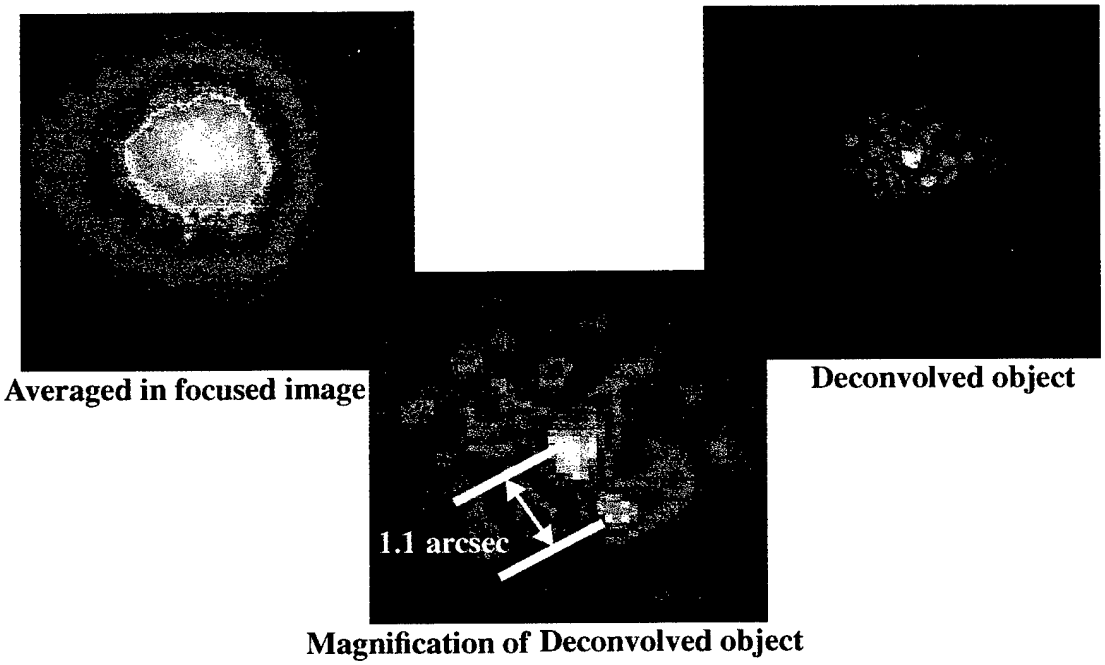

Figure(8) Original image, deconvolved object, and maginfication of deconvolved object.

5.0 CONCLUSIONS

The method of Phase Diversity can be used as a Wave Front Sensor to extract the optical aberrations present in the optical system. The error metric developed by Gonsalves, coupled with the method of conjugate gradient, is very robust and results in favorable solutions. The method was tried in experimental data and found to yield acceptable results. More analysis is needed to determine appropriate stopping criterion and convergence parameters, using the conjugate gradient method.

The technique of conjugate gradient is iterative in methodology and thus not fast enough to be used in a closed loop adaptive optics application. Work should proceed in finding faster and more efficient ways to increase the speed of this method. Some possible solutions are to parallelize the

procedure in order to solve for each aberration in a single computer. Other methods are to implement Phase Diversity using neural networks or fuzzy logic. This could yield substantial increase in speed.

5.0 REFERENCES

[1] •Paxman, R. G., Fienup, J. R., Optical Misalignment Sensing and Image Reconstruction Using Phase Diversity, J. Opt. Soc Am. A/Vol. 5, No. 6, June 1988

[2] •Paxman, R. G., Schulz, T. J.,Fienup, J. R., Joint estimation of Object and Aberrations by Using Phase Diversity, J. Opt. Soc Am. A/Vol. 9, No. 7, July 1992

[3] •Gaskill, J.D., Linear Systems, Fourier Transforms and Optics, John Wiley and Sons. New York

[4] •Goodman, J.R., Introduction to Fourier Optics, McGraw-Hill, N.Y

[5] •Gonsalves, R. A., Phase Retrieval From Modulus Data, J. Opt. Soc Am. Vol. 66, No. 9, September 1976

[6] •Gonsalves, R. A., Chidlaw, R., Wavefront Sensing by Phase Retrieval, SPIE. Vol. 207, Applications of Digital Image Processing III,1979

[7] •Gonsalves, R. A., Phase Retrieval and Diversity in Adaptive Optics, Optical Engineering, Vol. 21, No. 5, September/October, 1982

DISTRIBUTION LIST

AUL/LSE Bldg 1405 - 600 Chennault Circle Maxwell AFB, AL 36112-6424	1cy
DTIC/OCP 8725 John J. Kingman Rd, Suite 0944 Ft Belvoir, VA 22060-6218	2cys
AFSAA/SAI 1580 Air Force Pentagon Washington, DC 20330-1580	1cy
PL/SUL 3550 Aberdeen Ave SE Kirtland AFB, NM 87117-5776	2cys
PL/HO 3550 Aberdeen Ave SE Kirtland AFB, NM 87117-5776	1cy
Official Record Copy PL/LIMS Attn: Dr. Richard A. Carreras Kirtland AFB, NM 87117-5776	10cys